The following article appeared in Surface and Interface Analalysis 2017; 49: 18-24; and may be found at: https://doi.org/10.1002/sia.6045

Research article

SURFACE and INTERFACE ANALYSIS

Received: 30 March 2016 Revised: 22 April 2016 Accepted: 22 April 2016 Published online in Wiley Online Library: 26 May 2016

(wileyonlinelibrary.com) DOI 10.1002/sia.6045

In situ ion beam sputter deposition and X-ray photoelectron spectroscopy (XPS) of multiple thin layers under computer control for combinatorial materials synthesis

Thomas A. Wilson,[a] Anders J. Barlow,[b] Michael L. Foster,[a] Mariela Bravo Sanchez,[b,c] Jose F. Portoles,[b] Naoko Sano,[b] Peter J. Cumpson[b]* and Ian W. Fletcher[b]

Deposition of ultra-thin layers under computer control is a frequent requirement in studies of novel sensors, materials screening, heterogeneous catalysis, the probing of band offsets near semiconductor junctions and many other applications. Often large-area samples are produced by magnetron sputtering from multiple targets or by atomic layer deposition (ALD). Samples can then be transferred to an analytical chamber for checking by X-ray photoelectron spectroscopy (XPS) or other surface-sensitive spectroscopies. The 'wafer-scale' nature of these tools is often greater than is required in combinatorial studies, where a few square centimetres or even millimetres of sample is sufficient for each composition to be tested. The large size leads to increased capital cost, problems of registration as samples are transferred between deposition and analysis, and often makes the use of precious metals as sputter targets prohibitively expensive. Instead we have modified a commercial sample block designed to perform angle-resolved XPS in a commercial XPS instrument. This now allows ion-beam sputter deposition from up to six different targets under complete computer control. Ion beam deposition is an attractive technology for depositing ultra-thin layers of great purity under ultra-high vacuum conditions, but is generally a very expensive technology. Our new sample block allows ion beam sputtering using the ion gun normally used for sputter depth-profiling of samples, greatly reducing the cost and allowing deposition to be done (and checked by XPS) *in situ* in a single instrument. Precious metals are deposited cheaply and efficiently by ion-beam sputtering from thin metal foils. Samples can then be removed, studied and exposed to reactants or surface treatments before being returned to the XPS to examine and quantify the effects.

Keywords: XPS; X-ray photoelectron spectroscopy; deposition; *in situ*; combinatorial

Introduction

Combinatorial Materials Synthesis (CMS)[1] is an increasingly used technique for producing specimens suitable for high-throughput materials screening. Typical deposition methods are pulsed laser deposition or physical vapour deposition under computer control[2,3] to give gradients or libraries[4] of material combinations for subsequent screening.[5] In some cases the aim is to create a series of different bulk compositions, but in others (which we will be concerned with here) the aim is to provide a gradient or library of *surface* composition. This is most relevant, for example, in the screening of potential heterogeneous catalysts or other applications where surface properties dominate. In these cases, to check the composition produced, X-ray photoelectron spectroscopy (XPS) can be a valuable technique for the analysis of the composition and electronic structure of layers. Most XPS information is gained from a region between the surface and a depth of around 5 nm or so. Historically XPS was extremely useful, amongst other techniques, in elucidating mechanisms of growth of materials deposited by physical vapour deposition (evaporation or sputtering) during the 1960s and 1970s. Even now, sputter deposition and XPS analysis *in situ* can be extremely valuable in studies of the deposition of novel materials. In our multi-user XPS facility at the UK National EPSRC XPS Users' Service (NEXUS)[6] our clients often

* *Correspondence to: Peter J. Cumpson, National EPSRC XPS User's Service (NEXUS), School of Mechanical and Systems Engineering, Newcastle University, Newcastle upon Tyne NE1 7RU, United Kingdom.*
E-mail: peter.cumpson@ncl.ac.uk

a *School of Mechanical and Systems Engineering, Newcastle University, Newcastle upon Tyne NE1 7RU, United Kingdom*

b *National EPSRC XPS User's Service (NEXUS), School of Mechanical and Systems Engineering, Newcastle University, Newcastle upon Tyne NE1 7RU, United Kingdom*

c *CINVESTAV-Unidad Querétaro, Libramiento Norponiente 2000, Real de Juriquilla, Querétaro Qro. 76000, México*

d *Departamento de Materiales Avanzados, IPICYT, Camino a la Presa San José 2055, C.P. 78216, San Luis Potosí, SLP, México*

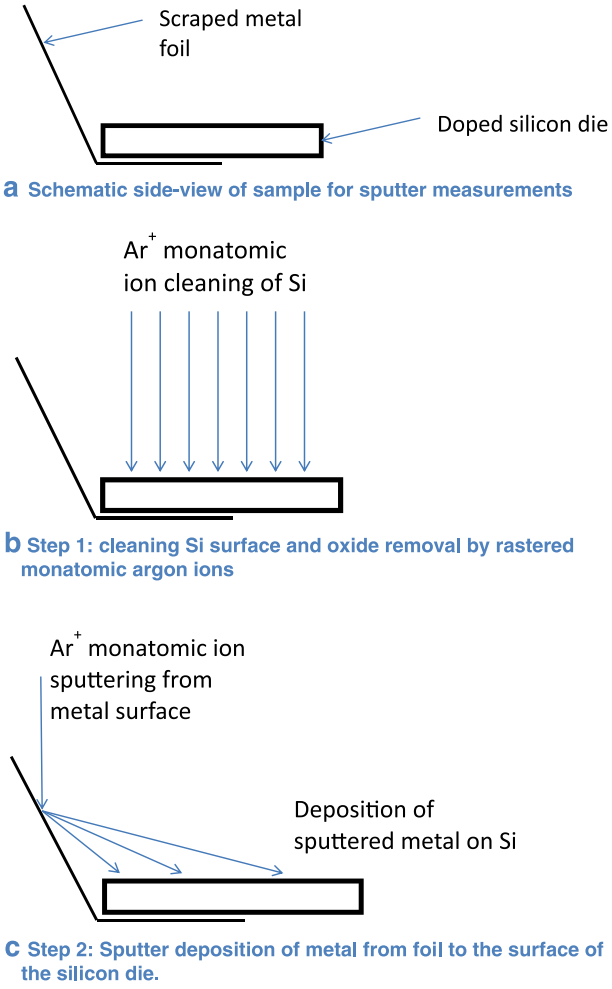

Figure 1. (a) Schematic side-view of sample for sputter measurements. (b) Step 1: cleaning Si surface and oxide removal by rastered monatomic argon ions. (c) Step 2: Sputter deposition of metal from foil to the surface of the silicon die.

need to deposit thin layers on samples or devices and then analyse the interface by XPS to determine the effect of the added layer. Nevertheless it is often expensive to incorporate flexible sputter deposition tools (for example including multiple target materials) with XPS instruments while ensuring that samples are not exposed to air in transfers between sputtering and analysis. Separate chambers for deposition and analysis mean expensive and potentially unreliable sample transfer and sample registration. What is more, sputter deposition tools are usually designed to deposit material rapidly over large areas, resulting in large sputter targets. The purchase of large sputter targets of precious metals (Pt and Au for example are frequent requirements) can be prohibitive. One recent study by a collaborator visiting our NEXUS XPS laboratory involved a series of sputtered films of materials including Pt and Au. This was part of a study of the effect of material composition on Schottky barrier height in semiconductor junctions. Precious metals were eliminated from this study simply because of material cost. Even for less expensive metals some of the materials involved were difficult to work and therefore expensive to purchase in the form of sputter targets.

In the past, to overcome the difficulties described above, we have had some success in depositing very thin films (<10 nm) from

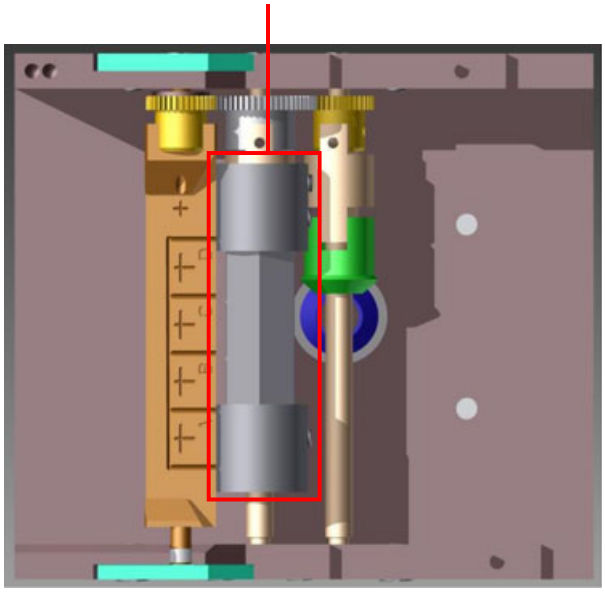

Figure 2. Top view of the CIMSIS sample block. The rotating sputter-target, hexagonal in cross-section, is outlined in red.

small pieces of metal foil *in situ* using an arrangement as shown schematically in Fig. 1. This is done in the analysis chamber of one of our XPS instruments. A small coupon of metal foil is folded to have an internal angle of about 110°, as shown in Fig. 1a. A beam of argon ions (clusters or monatomic as appropriate) is used to first clean the surface to be coated (for example the silicon die shown in Fig. 1b) and the metal foil sputter target. The same argon ion gun is then used to focus monatomic argon ions at the target Pt foil surface and sputter metal from the foil onto the silicon die. This technique was used by one of the authors, many years ago, to sputter Pt–10%Ir alloy onto the surface of a quartz crystal sensor.[7] Samples can then be removed, studied and exposed to reactants or surface treatments before being returned to the XPS to examine and quantify how the thickness or composition of deposited layers affects those reactants or treatments.

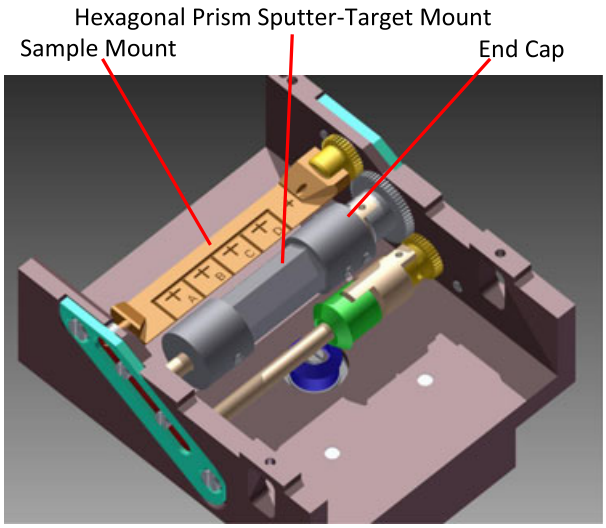

Figure 3. Perspective view of the CIMSIS sample block shown in Fig. 1.

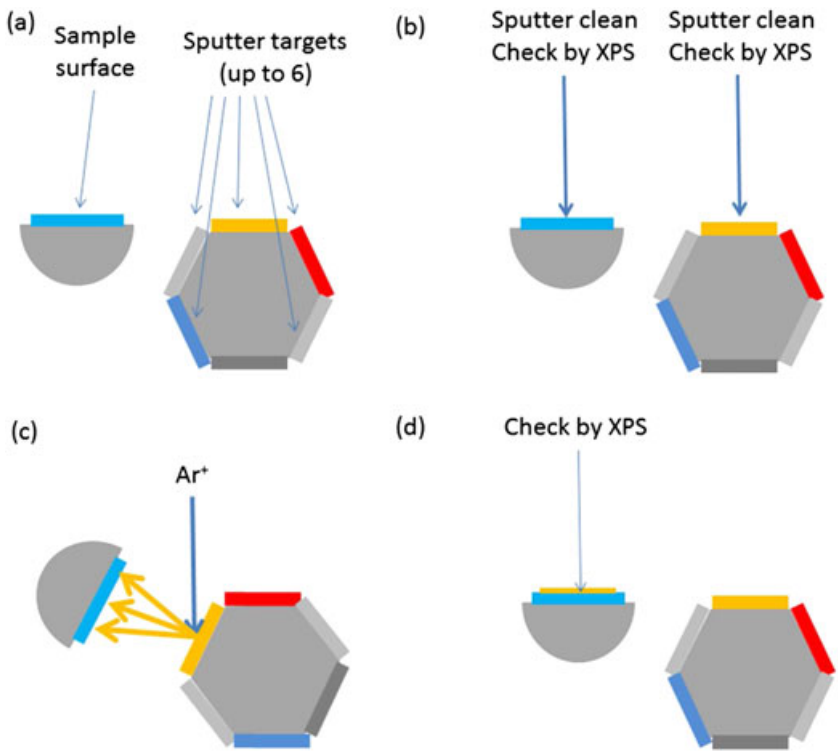

Figure 4. Schematic diagram illustrating a vertical cross section through the ion-beam sputter deposition arrangement *in situ* in our XPS instrument. (a) The Sample Mount and Hexagonal Prism Sputter Target Mount (b) Cleaning of sample and sputter target. Both are then rotated into an orientation favourable for sputter deposition, as shown in (c). Rotating both to their original orientations allows XPS to be used to check the composition and thickness of the deposited film. These steps are set out in detail in the section 'Computer control' on computer control of ion beam deposition.

Although we have been successful in deposition of metal in this way there are two important limitations that we will overcome in this paper:

a The sputter geometry shown in Fig. 1 is not optimal, so that much of the sputtered metal does not reach the surface where we wish it to be deposited.
b One can only easily deposit a single material in this way (though surrounding a silicon die with two or three pieces of metal foil may be possible *in extremis*, it becomes quite a clumsy arrangement if one is to have line-of-sight access from the ion gun to all targets).

We have therefore developed a device to allow up to six different materials to be deposited in a geometry that is much more advantageous in terms of sputter rate. We call this device CIMSIS—Combinatorial Ion-beam Material Sputtering *In Situ*.

CIMSIS is based on a modified commercial sample block for the Thermo K-Alpha XPS spectrometer (Thermo Scientific Ltd, East Grinstead, UK), although other manufacturers also offer tilt stages that could be modified in a very similar way. CIMSIS has the advantage of being inexpensive, but has much wider benefits too, notably the high purity of ion beam sputter deposition, the ultra-high vacuum conditions pertaining during deposition and the ability to clean surfaces (both the sputter target and deposition surface) with

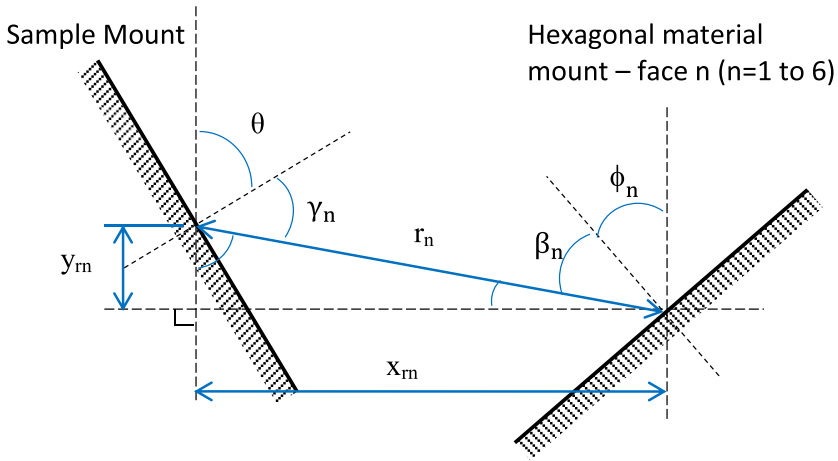

Figure 5. Sketch defining the geometry of sputtering in the CIMSIS device.

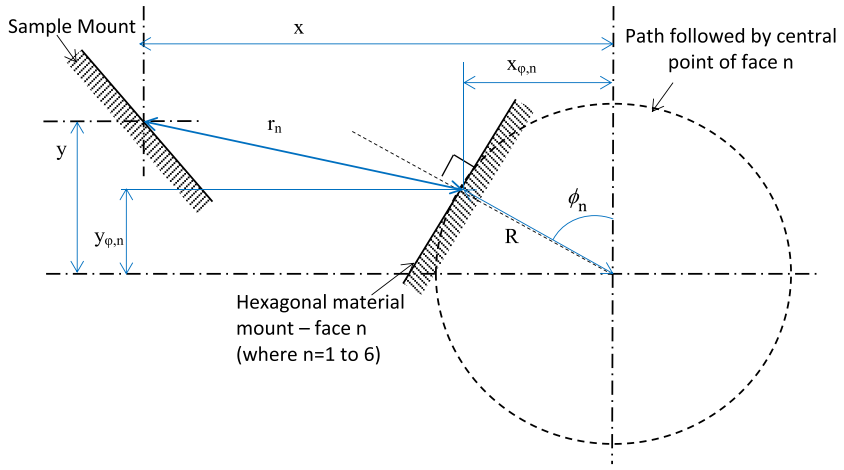

Figure 6. Cross section of hexagonal material mount in datum position.

advanced ion beams such as argon gas clusters[8–12] prior to deposition. All deposition methods have limitations, and the limitation of CIMSIS is the small amount of material that can be deposited in practice without undue time or wear-and-tear on the argon sputter gun – typically below 10 nm in thickness. This may make the method uncompetitive with other techniques (such as pulsed laser ablation[13]) in many applications, but on the other hand, if XPS is the technique chosen to characterise these surfaces it is likely that the minimum deposition thickness is roughly the same as the XPS sampling depth – in other words CIMSIS is ideally suited to studies in which the behaviour of the top few nanometres or so is being studied and where XPS one of the key characterisation techniques to be used in those studies.

The CIMSIS sample block

Several XPS instrument manufacturers make available a 'tilt block' to allow Angle-Resolved XPS[14] within their instruments. These convert a rotational motion about a vertical axis (provided to allow 'Zalar rotation'[15,16] of a sample during sputter depth profiling) into rotational motion about a horizontal axis. Samples attached to this rotating sample holder can then be tilted with respect to the vertical and allow XPS spectra to be acquired at specific angles under computer control. A gear system is used to convert the azimuthal rotation to a horizontal tilting motion. Figures 2 and 3 show rendered Computer-Aided Design (CAD) images of one such sample block after modification to produce a CIMSIS device. The important addition to make the CIMSIS device is the hexagonal prism sputter-target mount. As can be seen clearly in Fig. 3, the gear wheel attached to the hexagonal prism sputter-target mount has a larger diameter than the gear wheel attached to the rotating sample holder. This means that rotating the sample mount by one full rotation brings a different face of the hexagonal prism to be closest to the sample holder.

The difference in gear ratios between the sample and hexagonal mount spindles allows different sputter targets to be presented, in a geometry advantageous to sputter deposition, to the sample to be coated. In the particular case of the Thermo K-Alpha tilt stage the gear ratio 5:3 was found between the hexagonal target mount and sample mount gears. Of course the XPS data acquisition software that normally runs this XPS instrument is not designed to switch between the different geometries needed for deposition and analysis using our redesigned block. Nevertheless, enough flexibility is present in the software to allow this, although using somewhat indirect commands designed for different purposes. For example, one feature of the software, known as point positioning, can be used to rotate the tilt module to a predetermined angle. We use such commands to move the hexagonal target mount to an angle suitable for sputtering from the *n*th target, where *n* can be 1 to 6. First we developed a model relating the azimuthal angular displacement, θ, applied to the block to the angular displacement of targets and sample about their horizontal axes. This model allows us to find optimal values of θ to be applied under software control to select whichever target is required. Figure 4 shows schematically the order of events during deposition. The purpose of the next section is to develop a geometrical model that allows us to place definite instrument parameters (notably θ) under computer control to perform each of the steps illustrated in Fig. 4.

Sputter position requirements

The analysis position, as shown in Fig. 4 (a), (b) and (d), in which the sample is horizontal, allows the mounted materials to be 'cleaned' to remove any carbon or oxidised material before

Table 1. Analysis positions with respect to the azimuthal angle θ

Face value [n]	Azimuthal sputter angle [θ_{an}] (°)
1	550
2	50
3	150
4	250
5	350
6	450

Table 2. Ideal sputter positions with respect to the azimuthal angle θ

Face value [n]	Azimuthal sputter angle [θ_{sn}] (°)
1	1200.1
2	110.7
3	821.8
4	1533.6
5	446.3
6	1159.8

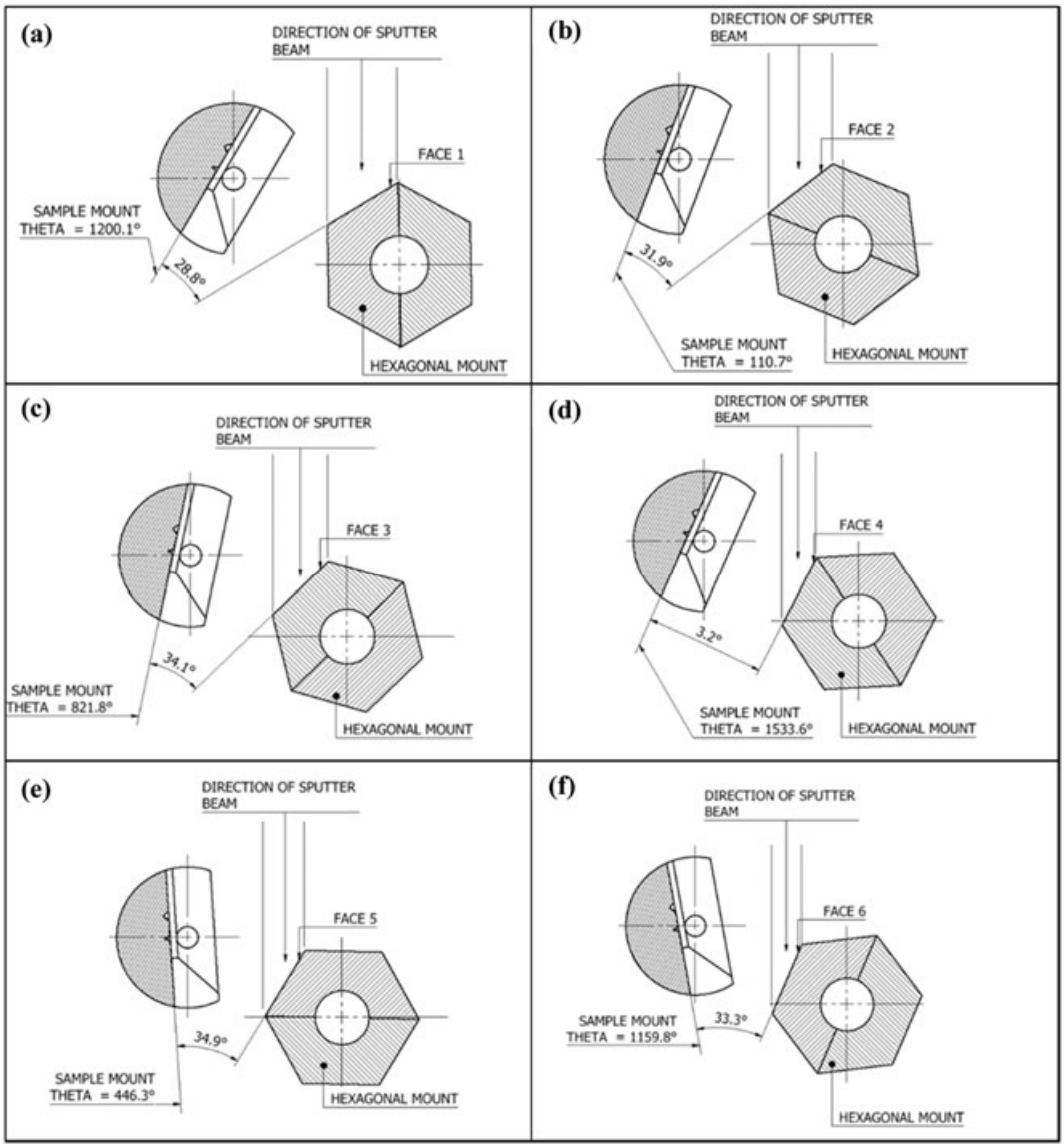

Figure 7. Sputter positions for the six faces. Because of the fixed gear ratio G the sputter geometry is favourable, although not identical, for sputtering from the six targets.

sputtering, and for that cleanliness to be checked by XPS. The objective then is to re-orientate the sputter target (chosen from one of the six sample materials on the hexagonal target holder) and the sample to be coated so as to achieve a favourable geometry and therefore a high sputter deposition rate. Below we analyse the sputter geometry in some detail so as to identify the optimum rotation.

Geometrical model

To find the azimuthal angles with the greatest sputtering rate per face, a line of sight relationship between the sample and material mount faces must be defined. Figure 5 defines the relevant angles and distances.

The angle of the normal to each of the six faces is φn, and the relationship between θ and ϕ_n is;

$$\varphi_n = G\cdot\theta + \alpha_n \quad (1)$$

where, in our specific sample block, the gear ratio $G = \frac{3}{5}$ and α_n is the initial angle of the nth face (and hence the nth sputter target). Clearly $\alpha_n = (n-1)\pi/3$ for faces of a regular hexagon. We approximate the arrival rate per unit area at the deposition sample as being proportional to the cosine of the sputter emission angle from the target, the cosine of the angle of incidence of the sputtered atoms with respect to the surface normal of the sample and the inverse-square of the distance between sputter target and sample.

$$\text{Sputter Rate} \propto \frac{1}{r^2}\cdot\cos(\beta)\cdot\cos(\gamma) \quad (2)$$

This allows us to define a 'figure-of-merit', the geometrical sputter efficiency (GSE*n*), in terms of the two angles and the line of sight length, r_n, from face *n* to the sample.

$$GSE_n = \frac{1}{r_n^2}\cdot\cos(\beta_n)\cdot\cos(\gamma_n) \quad (3)$$

Because of the gearing of the two axes of rotation the system has, in fact, only a single degree-of-freedom, so r_n, γ_n and β_n are

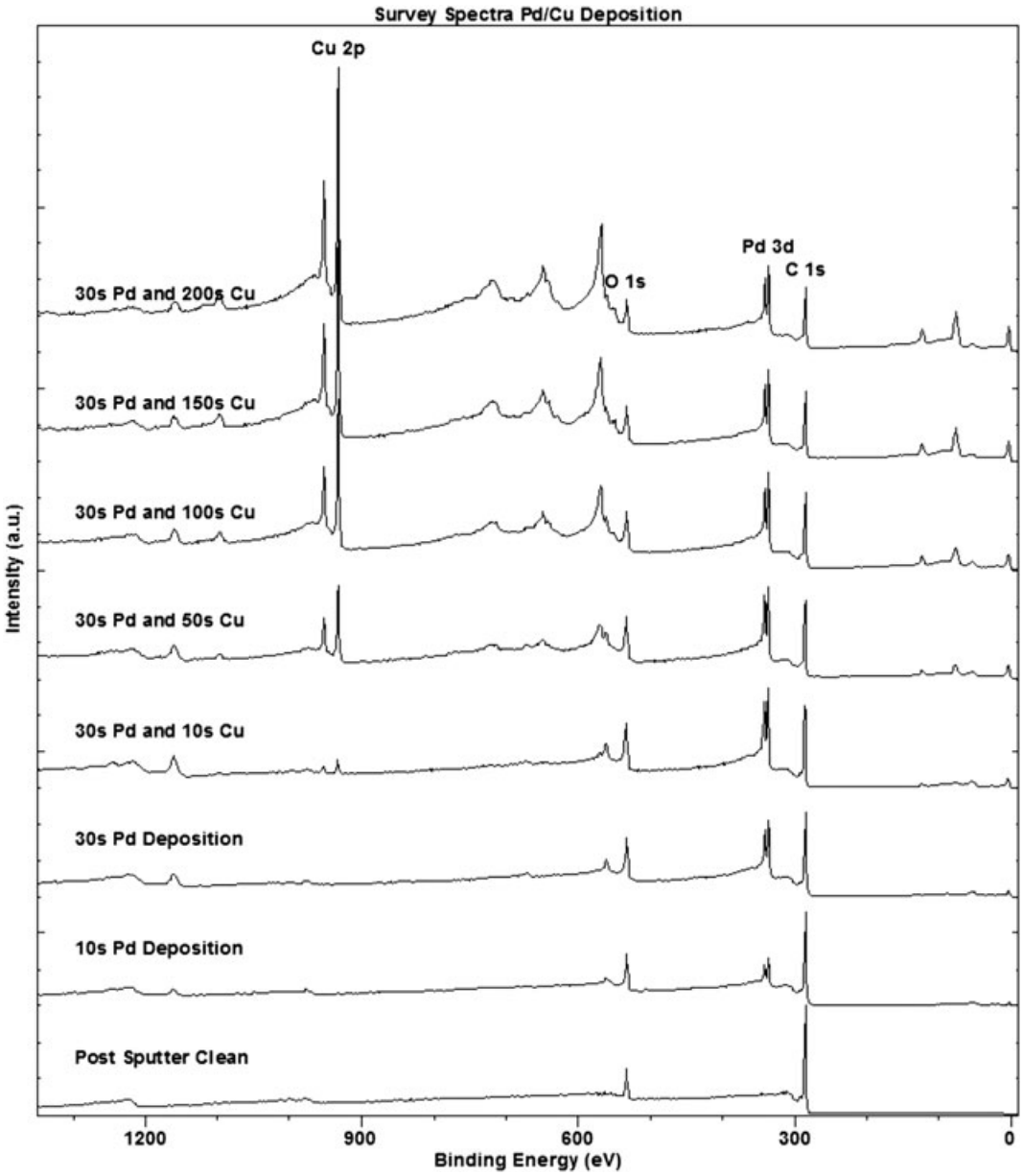

Figure 8. XPS spectra recorded during deposition *in situ*, progressing from bottom to top.

all functions of the angle θ. We can therefore identify the optimum sputter positions as stationary points in the function GSE with respect to that degree-of-freedom (Fig. 6).

$$r_n = \sqrt{\left((y - R\cdot\sin(\varphi_n))^2 + (x - R\cdot\cos(\varphi_n))^2\right)} \qquad (4)$$

A line of sight is only achieved when the cosine of both β_n, and α_n are positive so that only stationary points in GSE_n where $(\beta_n) \geq 0$ and $\cos(\gamma_n) \geq 0$ are used. To find the values of θ providing maximum values of GSE_n, we differentiated GSE_n with respect to θ and found those values at which the derivative is zero. Tables 1 and 2 show the θ values that provide the analysis and most effective sputter positions respectively. Figure 7 shows the final sputter positions.

Analysis Positions, Where θ_{an} is the analysis azimuthal angle for face n; **Sputter Positions**, Where θ_{sn} is the analysis azimuthal angle for face n

It can be seen in Fig. 7 that each face has a slightly different sputter position with respect to both the hexagonal and sample mounts. Were we to design the sample block from scratch (rather than adapt an existing Angle-Resolved XPS sample block as we have done) then the gear ratio would be under our control and we could choose a value that ensured an identical geometry between sputter target and sample whichever of the six targets is chosen for sputtering. As it is, the angle between target and sample is very slightly different for each of the six, but this has a negligible effect on the sputter rate given that it is the cosine of these angles that is significant for sputtering and in each case these angles are small.

The largest uncertainties that occur when sputtering with the CIMSIS are introduced by the mechanical components of its operation. There can be up to 10° of hysteresis in θ, because of the tilt module gearing, introduced when rotating alternately in positive and negative θ directions. To minimise the effects of hysteresis, the drive is only rotated in one direction, i.e. increasing θ.

Programming the Thermo Avantage commands to only rotate the block in a single direction reduces the hysteresis to below 5°.

Computer control

As with all modern XPS instruments the K-Alpha instrument operates under computer control, with analysis positions and spectra to be acquired being defined by the proprietary Avantage software package (Thermo Scientific, East Grinstead, UK). Sample position, as defined in this software, comprises *x*, *y* and *z* coordinates as well as the azimuthal rotation angle θ. We can make more definite the steps shown in Fig. 4 in the nine steps shown below, which have been transcribed into steps within the Avantage experiment file.

1 Move to sputter target *n* with target horizontal.
2 Sputter clean target using Ar cluster ions (to remove carbonaceous contamination) possibly followed by monatomic argon sputtering (for example to remove any oxide).
3 Check target cleanliness by XPS in situ.
4 Move to sample with sample horizontal.
5 Sputter clean sample using Ar cluster ions (to remove carbonaceous contamination), followed by monatomic argon sputtering (only if the damage introduced by these monatomic ions is acceptable).
6 Check sample cleanliness by XPS.
7 Rotate sample and target to one of the positions shown in Fig. 7, appropriate to sputtering from target *n*.
8 Sputter from the target using monatomic argon, usually at a high beam current setting.
9 Move to the sample with the sample horizontal and check surface composition by XPS.

This process is entirely automated as a scripted procedure within the Avantage software. It can be repeated to sputter deposit a sequence of layers chosen at will from the six available foils mounted on the hexagonal prism. Sputter times for cleaning often need some adjustment, but the ability to use both cluster and monatomic ions for sputtering within the K-Alpha instrument allows carbonaceous contamination to be removed preferentially[17] and this helps somewhat. The thickness of deposited layers is controlled by adjusting the sputter time in step 8.

Specimen sputter deposition results

To demonstrate the results of the automated deposition process Fig. 8 shows XPS spectra acquired during deposition of palladium and then copper on a sample of Polyether ether ketone (PEEK). All materials were obtained from Goodfellow Materials Ltd (Huntingdon, UK). The palladium and copper sputter targets were coupons pure metal foils around 5 mm × 5 mm × 125 μm thick, and mechanically attached to the hexagonal prism by having one corner placed under the endcap illustrated in Fig. 3. Each spectrum in the montage shown in Fig. 8 represents the XPS spectrum after an entire iteration of the steps 1 to 9 listed in the section Computer control above. Two iterations of Pd deposition were followed by five iterations of Cu deposition, so that (including an initial spectrum from PEEK) Fig. 8 shows eight spectra in total. These spectra show clean deposition of Pd and Cu without detectable oxidation or carbonaceous contamination (which would be expected were the sample to have to come out of vacuum between deposition steps).

We are currently working on the incorporation of a photochemically etched mesh in the CIMSIS device. This will allow the deposition of complex composition gradients across the sample surface, providing a tool capable of true combinatorial deposition.

Acknowledgements

X-ray photoelectron spectroscopy (XPS) data was acquired at the National EPSRC XPS Users' Service, an EPSRC Mid-Range Facility. Dr Mariela Bravo Sanchez wishes to thank Consejo Nacional de Ciencia y Tecnología (CONACYT), Mexico, for funding for her visiting researcher position at Newcastle University. The authors are grateful to Dr Tim Nunney of Themo Fisher Scientific for advice and information regarding the K-Alpha tilt block. Some of the instruments used in this work were purchased under an instrument package funded by EPSRC's 'Great Eight' capital funding grant EP/K022679/1 and Newcastle University, for which the authors are very grateful.

References

[1] X.-D. Xiang, I. Takeuchi (Eds), *Combinatorial Materials Synthesis*, Marcel Dekker, New York, USA, **2003**.
[2] B. Jandeleit, D. J. Schaefer, T. S. Powers, W. Howard, W. Turner, H. Weinberg, *Angew. Chem. Int. Ed.* **1999**, *38*(17), 2494–2532.
[3] X.-D. Xiang, *Annual Rev. Mater. Sci.* **1999**, *29*, 149–171.
[4] R. Potyrailo, K. Rajan, K. Stoewe, I. Takeuchi, B. Chisholm, H. Lam, *ACS Comb. Sci.* **2011**, *13*, 579–633.
[5] W. F. Maier, K. Stoewe, S. Sieg, *Angew. Chem. Int. Ed.* **2007**, *46*, 6016–6067.
[6] See www.ncl.ac.uk/nexus. [Accessed 5 May 2016]
[7] P. J. Cumpson, M. P. Seah, *Metrologia* **1996**, *33*, 507.
[8] N. Toyoda, H. Kitani, N. Hagiwara, J. Matsuo, I. Yamada, *Mater. Chem. Phys.* **1998**, *54*, 106–110.
[9] I. Yamada, J. Matsuo, N. Toyoda, A. Kirkpatrick, Materials processing by gas cluster ion beams, *Mater. Sci. Eng. R Rep.* **2001**, *34*(6), 231–295.
[10] P. J. Cumpson, J. F. Portoles, N. Sano, *Surf. Interface Anal.* **2013**, *45*, 601–604.
[11] P. J. Cumpson, J. F. Portoles, A. J. Barlow, N. Sano, *J. Appl. Phys.* **2013**, *114*, 124313.
[12] P. J. Cumpson, J. F. Portoles, N. Sano, *J. Vac. Sci. Technol. A* **2013**, *31*, 020605.
[13] D. A. Keller, A. Ginsburg, H.-N. Barad, K. Shimanovich, Y. Bouhadana, E. Rosh-Hodesh, I. Takeuchi, H. Aviv, Y. R. Tischler, A. Y. Anderson, A. Zaban, *ACS Comb. Sci.* **2015**. DOI:10.1021/co500094h.
[14] P. J. Cumpson, *J. Electron Spectros. Relat. Phenom* **1995**, *73*, 25–52.
[15] A. Zalar, *Thin Solid Films* **1985**, *124*, 223.
[16] M. M. Henneberg, D. J. Pocker, M. A. Parker, *Surf. Interface Anal.* **1992**, *19*, 55–59.
[17] P. J. Cumpson, J. F. Portoles, A. J. Barlow, N. Sano, M. Birch, *Surf. Interface Anal.* **2013**, *45*, 1859–1868.